J. Fluid Mech. (2017), *vol.* 830, R4, doi:10.1017/jfm.2017.649

JFM RAPIDS
journals.cambridge.org/rapids

Turbulent planar wakes under pressure gradient conditions

Sina Shamsoddin[1] **and Fernando Porté-Agel**[1,†]

[1]École Polytechnique Fédérale de Lausanne (EPFL), Wind Engineering and Renewable Energy Laboratory (WIRE), EPFL-ENAC-IIE-WIRE, CH-1015 Lausanne, Switzerland

(Received 13 July 2017; revised 10 August 2017; accepted 8 September 2017;
first published online 5 October 2017)

Accurate prediction of the spatial evolution of turbulent wake flows under pressure gradient conditions is required in some engineering applications such as the design of high-lift devices and wind farms over topography. In this paper, we aim to develop an analytical model to predict the evolution of a turbulent planar wake under an arbitrary pressure gradient condition. The model is based on the cross-stream integration of the streamwise momentum equation and uses the self-similarity of the mean flow. We have also made an experimentally supported assumption that the ratio of the maximum velocity deficit to the wake width is independent of the imposed pressure gradient. The asymptotic response of the wake to the pressure gradient is also investigated. After its derivation, the model is successfully validated against experimental data by comparing the evolution of the wake width and maximum velocity deficit. The inputs of the model are the imposed pressure gradient and the wake width under zero pressure gradient. The model does not require any parameter tuning and is deemed to be practical, computationally fast, accurate enough, and therefore useful for the scientific and engineering communities.

Key words: general fluid mechanics, mathematical foundations, wakes

1. Introduction

A better understanding of turbulent wakes under different pressure gradient scenarios is beneficial from both an engineering and a pure fluid mechanics point of view. As examples of engineering domains in which this phenomenon is involved, one can mention the aerodynamics of high-lift devices and also the wake structure and recovery in wind farms over hilly terrain. In high-lift devices, which are used in modern airliners, the wing is composed of several components, around which the air flows. The wake of the upstream components (e.g. the leading edge slat) has a crucial effect on the performance of the downstream components (e.g. the main wing

† Email address for correspondence: fernando.porte-agel@epfl.ch

and the flap(s)). These wakes are typically under strong (mainly adverse) pressure gradient conditions (Smith 1975; Rumsey & Ying 2002). Therefore, accounting for the pressure gradient effects for such wakes is decisive in the design of such systems. Wind-turbine wakes over hilly terrain (unlike flat terrain) also undergo non-zero pressure gradients and this affects their recovery rate and, consequently, the optimum design of modern wind farms over topography.

Several interesting studies have been performed on the subject at hand. Nakayama (1987) studied the effects of both pressure gradient and streamline curvature on mean flow and turbulence statistics of turbulent planar small-defect wakes. Liu, Thomas & Nelson (2002) performed a systematic and rigorous experimental investigation on the effect of pressure gradient on turbulent planar wakes. They observed that the wake velocity deficit recovers faster in the favourable pressure gradient case, and slower in the adverse pressure gradient case. They also conducted a detailed analysis on how and why the pressure gradient affects the wake flow in such a manner. The same group carried out a similar experimental investigation, but this time for asymmetric wakes in Thomas & Liu (2004). An interesting finding in both experiments is the fact that the ratio of the maximum velocity deficit to the wake width was 'virtually identical for each pressure gradient case', i.e. this ratio was invariant under different pressure gradient values. Rogers (2002) performed direct numerical simulations (DNS) of temporally strained planar wakes and did a thorough analysis of the self-similarity behaviour of the wake flow in strained conditions. He concluded that classical self-similarity leads to results which do not match those of DNS, and he developed a modified similarity formulation for strained wakes, which is mainly based on the fact that the growth of the wake width is determined by the straining. In that study, different rates and geometries (planar and axisymmetric) of strain are studied. One conclusion of his work was that the shape of the velocity deficit profile is universal in all strain geometries and values, and this shape is the same as that of an unstrained wake.

The objective that we pursue in this paper is to develop an analytical model to predict the evolution of a turbulent planar wake under an arbitrary pressure gradient condition. Specifically, we aim to predict how a turbulent planar wake in zero pressure gradient, which has a well-established behaviour, is perturbed by imposing a non-zero pressure gradient. The model is based on the cross-stream integration of the streamwise momentum equation and uses the self-similarity of the mean flow. The model proves to be computationally fast and easy to use for engineering and scientific purposes.

This article is structured as follows: the proposed model, with all its variants, is derived in § 2. The model is then validated against experimental data in § 3. A discussion about the effect of pressure gradient on turbulent planar wakes in a broader perspective is given in § 4, and the paper is concluded with § 5.

2. Analytical model for wakes under pressure gradient

2.1. *Problem formulation*

It is accepted that turbulent wakes behave in a self-similar manner under zero pressure gradient conditions (Tennekes & Lumley 1972; Wygnanski, Champagne & Marasli 1986; Pope 2000). It has also been shown that turbulent wakes preserve their self-similar behaviour in the mean streamwise velocity under non-zero pressure gradient (or strained) conditions (Liu *et al.* 2002; Rogers 2002; Thomas & Liu 2004). A schematic of key variables in a turbulent planar wake is shown in figure 1.

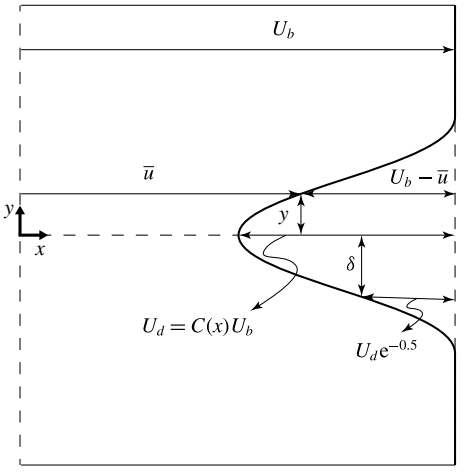

FIGURE 1. Schematic of the velocity profile of a typical turbulent planar wake.

As it can be seen, x is the streamwise direction, y is the lateral direction, the x-axis is coincident with the centreline of the wake, $\overline{u}(x, y)$ is the velocity (hereafter, by velocity, we imply the mean streamwise velocity, unless otherwise stated) of the wake flow, $U_b(x)$ is the velocity of the base flow, i.e. the velocity of the flow assuming there is no wake (in other words, $U_b(x) = \lim_{|y|\to\infty} \overline{u}(x, y)$). We can express the velocity self-similarity of the wake as:

$$\frac{U_b - \overline{u}}{U_b} = C(x) f(y/\delta), \tag{2.1}$$

where $C(x)$ is a function determining the maximum velocity deficit at each x-position, $\delta(x)$ is a length scale in the y-direction and $f(y/\delta)$ is a shape function that describes the shape of the velocity profile. It is also already shown that the shape function for turbulent wakes under zero (Wygnanski *et al.* 1986; Pope 2000) and non-zero (Liu *et al.* 2002; Rogers 2002) pressure gradients can be expressed by a Gaussian function. Thus, for a planar wake we have:

$$\frac{U_b - \overline{u}}{U_b} \equiv C(x) e^{-y^2/2\delta^2}. \tag{2.2}$$

In fact, the profile proposed by Wygnanski *et al.* (1986) has also a term involving $\exp(y^4)$, which can be, to a good accuracy, neglected (Rogers 2002).

With this representation of the wake velocity, $\delta(x)$ can be regarded as the wake width. The wake width for the zero pressure gradient case $\delta_0(x)$ is determined by the geometry of the wake-generating object and the incoming turbulence level of the flow. For example, it is known that for a planar wake and a laminar inflow $\delta_0(x) \sim x^{1/2}$. Depending on the turbulence level of the inflow and the geometry of the object, this relation is subject to change.

We now state the problem that we want to solve. The problem is: assuming the wake width for the zero pressure gradient case is given, it is desired to find the maximum deficit function $C(x)$ (including C_0) and $\delta(x)$ under any given pressure gradient. In other words, we want to be able to analytically predict how the wake

flow changes, with respect to the zero pressure gradient one, for different pressure gradient conditions.

In the above formulation, the pressure gradient ($\mathrm{d}\overline{p}/\mathrm{d}x$) shows itself in the way the base flow velocity U_b varies with x, i.e. if we have a base flow acceleration ($\mathrm{d}U_b/\mathrm{d}x > 0$) then $\mathrm{d}\overline{p}/\mathrm{d}x < 0$, and we have the so-called favourable pressure gradient (FPG) condition; alternatively, if we have a base flow deceleration ($\mathrm{d}U_b/\mathrm{d}x < 0$) then $\mathrm{d}\overline{p}/\mathrm{d}x > 0$, and we have the so-called adverse pressure gradient (APG) condition. For the zero pressure gradient (ZPG) case, we have $U_b(x) = U_{b0} = \text{const}$.

2.2. *Model derivation*

We start with the mean momentum conservation equation in the x-direction for a two-dimensional planar turbulent flow:

$$\overline{u}\frac{\partial \overline{u}}{\partial x} + \overline{v}\frac{\partial \overline{u}}{\partial y} = -\frac{1}{\rho}\frac{\partial \overline{p}}{\partial x} - \frac{\partial \overline{u'v'}}{\partial y} - \frac{\partial \overline{u'^2}}{\partial x}, \tag{2.3}$$

where u and v are the streamwise and lateral components of velocity, p is the pressure, ρ is the fluid density, the overbar indicates a mean quantity and the prime shows the fluctuation quantities (e.g. $u' = u - \overline{u}$). Here, we have already neglected viscous effects as the Reynolds number is taken to be sufficiently high. As the variation of the turbulent fluxes in the streamwise direction is negligible, the last term on the right-hand side of the above equation can also be neglected. The pressure gradient term can be written as $U_b(\mathrm{d}U_b/\mathrm{d}x)$. With these considerations and adding the term $-\overline{u}\,\mathrm{d}U_b/\mathrm{d}x$ to both sides of (2.3), we can rewrite this equation in the following form:

$$\overline{u}\frac{\partial (U_b - \overline{u})}{\partial x} + \overline{v}\frac{\partial (U_b - \overline{u})}{\partial y} = \frac{\partial \overline{u'v'}}{\partial y} - U_b\frac{\mathrm{d}U_b}{\mathrm{d}x} + \overline{u}\frac{\mathrm{d}U_b}{\mathrm{d}x}. \tag{2.4}$$

Using continuity, we obtain:

$$\frac{\partial \overline{u}(U_b - \overline{u})}{\partial x} + \frac{\partial \overline{v}(U_b - \overline{u})}{\partial y} = \frac{\partial \overline{u'v'}}{\partial y} - \frac{\mathrm{d}U_b}{\mathrm{d}x}(U_b - \overline{u}). \tag{2.5}$$

Now, we integrate the above equation in the y-direction. As both $(U_b - \overline{u})$ and $\overline{u'v'}$ vanish far from the wake centre, the following equation is yielded:

$$\frac{\mathrm{d}}{\mathrm{d}x}\int_{-\infty}^{\infty} \overline{u}(U_b - \overline{u})\,\mathrm{d}y + \int_{-\infty}^{\infty}\frac{\mathrm{d}U_b}{\mathrm{d}x}(U_b - \overline{u})\,\mathrm{d}y = 0. \tag{2.6}$$

As can be noticed, the second term on the left-hand side of the equation is responsible for the pressure gradient effect. In the special case of the zero pressure gradient case, the second term will be equal to zero, and the above equation is reduced to the well-known momentum defect equation for turbulent wakes (Tennekes & Lumley 1972). Plugging (2.2) into (2.6), and using $\int_{-\infty}^{\infty}\exp[-y^2/(2\delta^2)]\,\mathrm{d}y = \sqrt{2\pi}\delta$, we obtain the following:

$$\frac{\mathrm{d}}{\mathrm{d}x}\left[\sqrt{\pi}U_b^2(x)\delta(x)(\sqrt{2}C(x) - C^2(x))\right] + \frac{1}{2}\sqrt{2\pi}\frac{\mathrm{d}U_b^2}{\mathrm{d}x}\delta(x)C(x) = 0. \tag{2.7}$$

As can be seen, in a zero pressure gradient case, the second term vanishes and we are left with an algebraic equation for $C(x)$ (the same as Bastankhah & Porté-Agel

(2014) for an axisymmetric wake). However, in the case of non-zero pressure gradient we encounter a nonlinear ordinary differential equation (ODE). We first solve the above equation for the ZPG case, as its solution will be useful later in our derivation. In the ZPG case, equation (2.7) reduces to:

$$\left[\sqrt{\pi}U_{b0}^2\delta_0(x)(\sqrt{2}C_0(x)-C_0^2(x))\right]=M, \tag{2.8}$$

where the 0 subscript indicates the ZPG case. The term on the left-hand side of the above equation is the net momentum deficit flux per unit density per unit spanwise (normal to the xy-plane) depth, and is equal to a constant (Tennekes & Lumley 1972). The value of this constant is related to the momentum flux removal by the wake-generating object, and it is equal to $M=(C_DDU_{b0}^2)/2$, where C_D is the drag coefficient of the wake-generating object and D is its width. Therefore, $C_0(x)$ is found to be:

$$C_0(x)=\frac{\sqrt{2}}{2}-\sqrt{\frac{1}{2}-\frac{C_D}{2\sqrt{\pi}\dfrac{\delta_0(x)}{D}}}\quad(x\geqslant x_i). \tag{2.9}$$

Note that $\delta_0(x)$ is treated as a known function, so with the above equation, $C_0(x)$ is fully determined. The condition $x\geqslant x_i$ is only to ensure that the expression under the square root is non-negative. Thus, x_i is equal to the minimum non-negative value of x, for which the expression under the square root remains non-negative.

We now turn back to (2.7), in which we have one equation and two unknowns (i.e. $C(x)$ and $\delta(x)$). Therefore, to be able to solve the problem we need another equation that relates $C(x)$ and $\delta(x)$. For this purpose, we define $\lambda(x)$ as:

$$\lambda(x)\equiv\frac{U_d}{\delta}, \tag{2.10}$$

where $U_d(x)\equiv C(x)U_b(x)$ is the maximum velocity deficit at a given streamwise position. Although both $U_d(x)$ and $\delta(x)$ vary with pressure gradient, it has been experimentally shown by Liu *et al.* (2002) and Thomas & Liu (2004) that $\lambda(x)$ is virtually invariant under pressure gradient changes. To explain this finding, they have argued that $\lambda(x)$ is proportional to the maximum of $\partial\overline{u}/\partial y$ and, hence, to the maximum of the mean normal-to-plane vorticity $\overline{\omega_z}$. As in the vorticity equation for $\overline{\omega_z}$, the imposed pressure gradient does not appear ($\boldsymbol{\nabla}\times\boldsymbol{\nabla}\overline{p}=0$), the imposed pressure gradient does not have a direct effect on the evolution of the maximum of $\overline{\omega_z}$. We take advantage of this, and further our derivation, by equating λ for any pressure gradient to the value of λ for the ZPG case, i.e. λ_0:

$$\lambda(x)=\lambda_0(x)=\frac{U_{b0}C_0(x)}{\delta_0(x)}, \tag{2.11}$$

which, considering (2.9), is regarded as a known function. $\delta(x)$ can then be expressed as:

$$\delta(x)=\frac{U_b(x)}{\lambda_0(x)}C(x). \tag{2.12}$$

Plugging (2.12) into (2.7), the following ODE is obtained for $C(x)$:

$$\frac{\mathrm{d}C(x)}{\mathrm{d}x}=\frac{-1}{\left(\dfrac{U_b^3}{\lambda_0}\right)(2\sqrt{2}C-3C^2)}\left[\frac{\sqrt{2}}{3}\frac{\mathrm{d}U_b^3}{\mathrm{d}x}\frac{C^2}{\lambda_0}+(\sqrt{2}C^2-C^3)\frac{\mathrm{d}}{\mathrm{d}x}\left(\frac{U_b^3}{\lambda_0}\right)\right]. \tag{2.13}$$

The boundary condition for the above ODE is:

$$C(x_i) = C_0(x_i). \tag{2.14}$$

In fact, by (2.14), we have assumed that $C(x)$ has the same initial value for both the ZPG and non-zero pressure gradient cases. In other words, in the immediate vicinity of the wake-generating object, the effect of pressure gradient on $C(x)$ is assumed to be negligible. This notion is fully accurate in cases where the imposed pressure gradient starts to be non-zero after some distance from the object (e.g. see the validation case of § 3).

Equation (2.13), which is nonlinear in $C(x)$, enables us to explicitly express $\mathrm{d}C(x)/\mathrm{d}x$ as a function of U_b, λ_0 and $C(x)$, i.e. $\mathrm{d}C(x)/\mathrm{d}x = f(U_b, \lambda_0, C)$. This form of the ODE is suitable for common numerical ODE solvers, and it can be solved very easily and fast. Hence, with (2.13) and (2.14), the solution of the initially stated problem (§ 2.1) is fully achieved. In the remainder of this section, we approach the problem from two other different angles, which we believe can shed more light on the problem at hand.

2.3. *Solving the problem for a given $\delta(x)$*

Herein, we consider the problem as such: $\delta(x)$ is given for a desired pressure gradient, and the objective is to find $C(x)$. This approach is beneficial because it disentangles (2.7) from (2.11), and we can isolate the behaviour of these two equations, and consequently assess them individually. This may be particularly useful for the insight it provides.

For this purpose, we proceed by defining a dummy variable $h(x)$ such that $h(x) \equiv \delta(x)(\sqrt{2}C(x) - C^2(x))$. Then, equation (2.7) becomes:

$$\frac{\mathrm{d}h(x)}{\mathrm{d}x} = -h(x)\frac{1}{U_b^2}\frac{\mathrm{d}U_b^2}{\mathrm{d}x} - \frac{\sqrt{2}}{2}\frac{1}{U_b^2}\frac{\mathrm{d}U_b^2}{\mathrm{d}x}\delta\left(\frac{\sqrt{2}}{2} - \sqrt{\frac{1}{2} - \frac{h}{\delta}}\right), \tag{2.15}$$

with the boundary condition being:

$$h(0) = h_0(x) = \frac{1}{2\sqrt{\pi}}DC_D. \tag{2.16}$$

The above ODE is nonlinear in $h(x)$ and has the explicit form $\mathrm{d}h(x)/\mathrm{d}x = f(U_b, \delta, h)$. Equation (2.15) can again be easily solved in a fast way by numerical techniques, which are available in common commercial softwares. Finally, $C(x)$ is recovered as:

$$C(x) = \frac{\sqrt{2}}{2} - \sqrt{\frac{1}{2} - \frac{h}{\delta}} \quad (x \geqslant x_i). \tag{2.17}$$

Note that $h(x)$ becomes independent of x in the ZPG case (2.16). Notice also that in the derivations of this section, wherever one of the two roots of a quadratic equation was needed ((2.9), (2.15) and (2.17)), the physically acceptable one was chosen, and the unacceptable one was ignored. The unacceptable root leads to negative flow velocity and an amplifying deficit in the x-direction instead of an attenuating one for the ZPG case.

2.4. *Asymptotic solution of the problem*

Here, we try to find an asymptotic solution for the problem at hand for sufficiently large x. To this end, we consider that $0 < C(x) < 1$, and thus $C^2(x) < C(x)$. We know that $C(x) \to 0$ as $x \to \infty$ (at least for ZPG and FPG cases, as we will see in § 3, this assumption does not necessarily hold for the APG case). Hence, in the far wake, where x is sufficiently large, we have $C^2(x) \ll C(x)$. Therefore, here we can consider the term involving $C^2(x)$ as negligible with respect to the term involving $C(x)$. Neglecting the $C^2(x)$, amounts to an important change in (2.7), that is to say, converting the nonlinear ODE to a linear one:

$$\frac{\mathrm{d}}{\mathrm{d}x}\left[\sqrt{2\pi}U_b^2(x)\delta\widetilde{C}(x)\right] + \frac{\sqrt{2\pi}}{2}\frac{\mathrm{d}U_b^2}{\mathrm{d}x}\delta\widetilde{C}(x) = 0, \tag{2.18}$$

where $\widetilde{C}$ is the asymptotic solution of C. After some manipulation, we obtain the following equation:

$$\sqrt{2\pi}\frac{1}{U_b}\frac{\mathrm{d}}{\mathrm{d}x}[\delta(x)\widetilde{C}(x)U_b^3] = 0. \tag{2.19}$$

The coefficient $\sqrt{2\pi}$ is maintained deliberately, so that the constant of integration for the above equation for the ZPG case will be equal to M in (2.8). The solution to the above equation can be obtained with the proper determination of the constant of integration. Thus, $\widetilde{C}(x)$ can be written as:

$$\widetilde{C}(x) = \frac{1}{2\sqrt{2\pi}}\frac{C_D}{\left(\dfrac{\delta}{D}\right)}\left(\frac{U_{b0}}{U_b(x)}\right)^3. \tag{2.20}$$

It is noteworthy to mention that the above expression in the case of ZPG (i.e. $\widetilde{C}_0(x) = 1/(2\sqrt{2\pi})DC_D/\delta_0$) is, in fact, equal to the first-order Taylor expansion of the full solution of $C_0(x)$, i.e. (2.9).

Now, using (2.11), we can find the final asymptotic solution for $C(x)$ as:

$$\widetilde{C}(x) = \widetilde{C}_0(x)\left(\frac{U_{b0}}{U_b(x)}\right)^2. \tag{2.21}$$

3. Validation of the model

In this section, we aim to validate the above-derived model by comparing its predictions with experimental measurements. The experiment that we choose is the one performed by Liu *et al.* (2002), in which the wake generated by a flat splitter plate under different constant pressure gradient conditions is measured. The pressure gradient along the streamwise direction has the following distribution:

$$\frac{\mathrm{d}C_p}{\mathrm{d}x} \equiv \frac{1}{\frac{1}{2}\rho U_{b0}^2}\frac{\mathrm{d}\overline{p}}{\mathrm{d}x} = -\frac{\mathrm{d}}{\mathrm{d}x}\left(\frac{U_b}{U_{b0}}\right)^2 = \begin{cases} 0, & x \leqslant x_p \\ \alpha, & x > x_p, \end{cases} \tag{3.1}$$

where C_p is the pressure coefficient. It is clear from the above distribution that the wake is initially under zero pressure gradient and, after a certain position x_p ($x_p/\theta_0 = 40$), it undergoes a constant pressure gradient which is dictated by the parameter α.

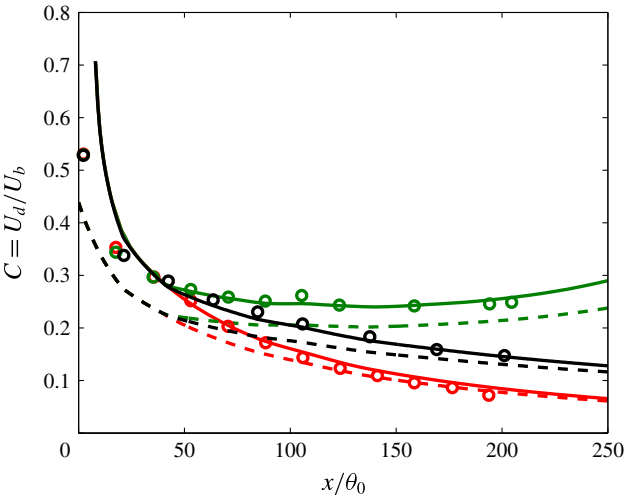

FIGURE 2. Normalized maximum velocity deficit as a function of the streamwise distance for ZPG (black), FPG (red) and APG (green) cases. The circles indicate measurements of Liu *et al.* (2002), the solid lines are the full solution obtained from (2.13), and the dashed lines are the asymptotic solution of (2.21).

θ_0 is the initial momentum thickness of the wake, which is equal to 7.2 mm for all the cases considered here. Three cases of ZPG, FPG and APG are considered, such that:

$$\alpha = \begin{cases} -0.6\ \mathrm{m}^{-1}, & \text{FPG} \\ 0, & \text{ZPG} \\ +0.338\ \mathrm{m}^{-1}, & \text{APG.} \end{cases} \tag{3.2}$$

We here apply the model described in § 2 to these three cases. Note that in the model one can use the wake half-width $\delta_h = \sqrt{2\ln(2)}\delta$ instead of δ, as (2.7) is linear in δ. The lengths are normalized by θ_0. Using the curve of $C_0(x)$ in the experiment, the value of the DC_D in (2.9) can be obtained, and this equation eventually takes the following form:

$$C_0(x) = \frac{\sqrt{2}}{2} - \sqrt{\frac{1}{2} - \frac{2.2}{2\sqrt{\pi}\left(\dfrac{\delta_{h,0}(x)}{\theta_0}\right)}}, \tag{3.3}$$

where $\delta_{h,0}$ is the wake half-width for the ZPG case.

Figure 2 shows $C(x) = U_d(x)/U_b(x)$ for the different pressure gradient cases both from the measurements and from the model. Along with the full solution of the model (i.e. (2.13)), the asymptotic solution is also shown. Note that, all ODEs in this paper are solved with '*ode45*' routine of MATLAB, which uses an explicit Runge–Kutta (4, 5) algorithm, namely, the Dormand–Prince method. The agreement between the model and the experimental data is remarkable. It is also clear how the asymptotic solution converges to the full solution for the ZPG and FPG cases. For the APG case, as the condition $\lim_{x\to\infty} C(x) = 0$ does not hold, we see that no convergence to the full solution is achieved. It is also worth mentioning that the asymptotic solution performs best for the FPG case, and this is because the value of $C(x)$ is the smallest for this case, and consequently, the error caused by neglecting $C^2(x)$ is also the smallest.

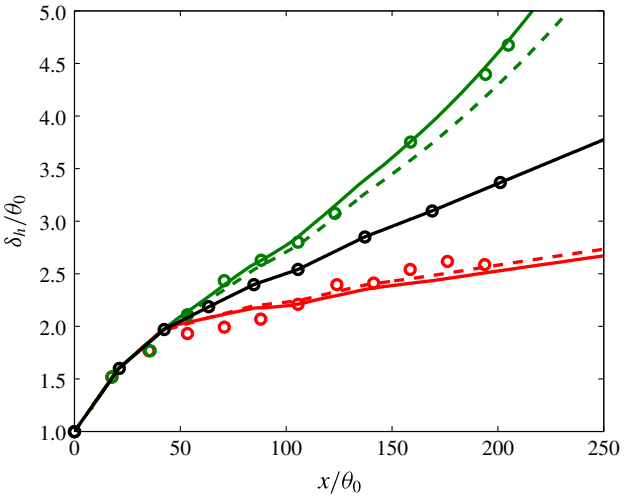

FIGURE 3. Normalized wake half-width as a function of the streamwise distance. For the legend, refer to the caption of figure 2.

It can be observed that the recovery of the maximum velocity deficit is fastest for the FPG case and slowest for the APG case. In fact, for the APG case, after a certain x, $C(x)$ even starts to increase. This is also reported by Liu *et al.* (2002), and it is well predicted by our model. Moreover, figure 3 shows the modelled and experimental $\delta_h(x)$ functions. Again, it can be seen that the agreement between the model and measurements is good. Note that the black line in this figure is the input of the model. This curve, as also reported by Liu *et al.* (2002), grows proportional to $x^{1/2}$.

4. Discussion

After validation of the model, we aim to employ the model to give us more insight about the response of planar wakes to pressure gradient conditions. To this end, we use the set-up presented in the previous section, and examine the behaviour of the wake with varying pressure gradients. To do this, we vary the parameter α and obtain the solutions of $C(x)$ and $\delta_h(x)$, as can be seen in figures 4 and 5, respectively. First of all, we see in these figures that, for the APG cases, there is a certain value of x/θ_0 beyond which the solution becomes unstable. We hypothesize that one possible reason for this behaviour can be the separation of the flow, which is reported broadly in literature as a characteristic of APG wakes. It is worth noting that Liu *et al.* (2002) have mentioned for $\alpha = 0.468$ m^{-1} the flow undergoes separation 'near the aft portion of the diffuser wall', i.e. $x/\theta_0 \approx 250$; interestingly, we observe in figures 4 and 5 that this agrees well with the point where the model becomes unstable. Moreover, for the case of constant adverse pressure gradient ($\alpha > 0$), the existence of a certain x at which the model becomes unstable does not depend on the magnitude of α. In the above figures, also for $\alpha = 0.1$ m^{-1} the model becomes unstable, but at $x/\theta_0 \approx 1000$, which is not within the range of the shown plots. We emphasize that linking the instability of the model to flow separation is only a hypothesis, and investigation of the separation is not within the scope of this study. Another interesting point about this figure is the fact that wakes under APG are more sensitive to pressure gradient than wakes under FPG; in contrast to FPG cases, the wake responds to a small APG relatively strongly.

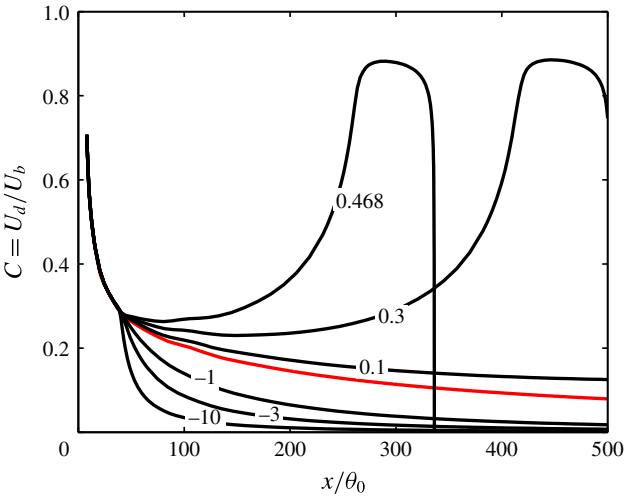

FIGURE 4. Normalized maximum velocity deficit as a function of the streamwise distance for different pressure gradient cases. The value of α is written on each curve with the unit of (m^{-1}). The red line indicates the ZPG case. The curves are the solution of (2.13).

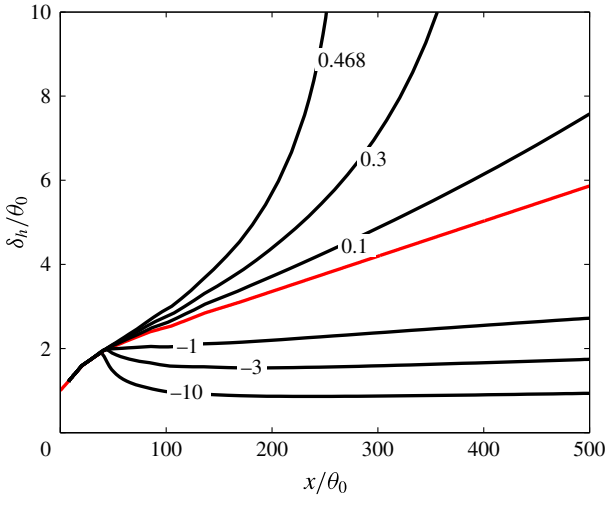

FIGURE 5. Normalized wake half-width as a function of the streamwise distance for different pressure gradient cases. For the legend, refer to the caption of figure 4.

Finally, we see that when the magnitude of the favourable pressure gradient is larger than a certain value (i.e. $\alpha < \alpha_{cr} < 0$), δ varies only slightly with x, i.e. $\delta \approx$ const. This means that the flow becomes close to a parallel flow. This behaviour is also mentioned by Liu *et al.* (2002) and Rogers (2002).

5. Concluding remarks

In this paper, we pursue the objective of developing an analytical model to predict the evolution of a turbulent planar wake under an arbitrary pressure gradient condition.

Specifically, we aim to predict how a turbulent planar wake in zero pressure gradient, which has a well-established behaviour, is perturbed by imposing a non-zero pressure gradient. The model is based on the cross-stream integration of the streamwise momentum equation and uses the self-similarity of the mean flow.

The inputs of the model are: (i) the ZPG wake width evolution function $\delta_0(x)$, and (ii) the imposed pressure gradient, or equivalently, the streamwise distribution of the base flow velocity $U_b(x)$. Both input functions can be data-driven or analytical. The outputs of the model are the maximum deficit function $C(x)$ and the wake width function $\delta(x)$. The model amounts to solving a nonlinear ODE for $C(x)$, which can be easily solved in a fast way with common commercial ODE solvers. An asymptotic variant of the model (mainly applicable for ZPG and FPG cases) is also developed which leads to an algebraic equation for $C(x)$. The asymptotic method was found to have no computational advantage over the exact method, but it can help to give a clearer insight about the problem. The model is successfully validated against experimental data by comparing the evolution of the wake width and maximum velocity deficit for both FPG and APG cases. The model is shown to be useful to predict a broad range of pressure gradients.

Finally, as mentioned in § 1, apart from high-lift devices, wind-turbine wakes can also involve pressure gradient effects. The main characteristic difference between these two cases is that the wake in high-lift devices is planar, but the wake of wind turbines is axisymmetric. The approach described here for planar wakes can easily be extended to axisymmetric wakes. Although this can be accomplished using a similar general approach, the results will be different and, therefore, a proper separate investigation of axisymmetric wakes under pressure gradient conditions is required. We are planning to undertake this challenge in our future research.

Acknowledgements

This research was supported by EOS (Energie Ouest Suisse) Holding, the Swiss Federal Office of Energy (grant SI/501337-01), the Swiss National Science Foundation (grant 200021_172538) and the Swiss Innovation and Technology Committee (CTI) within the context of the Swiss Competence Center for Energy Research 'FURIES: Future Swiss Electrical Infrastructure'. We also thank Dr M. Bastankhah for his kind and thorough check of the final version of the manuscript.

References

BASTANKHAH, M. & PORTÉ-AGEL, F. 2014 A new analytical model for wind-turbine wakes. *J. Renew. Energy* **70**, 116–123; special issue on aerodynamics of offshore wind energy systems and wakes.

LIU, X., THOMAS, F. O. & NELSON, R. C. 2002 An experimental investigation of the planar turbulent wake in constant pressure gradient. *Phys. Fluids* **14** (8), 2817–2838.

NAKAYAMA, A. 1987 Curvature and pressure-gradient effects on a small-defect wake. *J. Fluid Mech.* **175**, 215–246.

POPE, S. B. 2000 *Turbulent Flows*. Cambridge University Press.

ROGERS, M. M. 2002 The evolution of strained turbulent plane wakes. *J. Fluid Mech.* **463**, 53–120.

RUMSEY, C. L. & YING, S. X. 2002 Prediction of high lift: review of present CFD capability. *Prog. Aerosp. Sci.* **38** (2), 145–180.

SMITH, A. M. O. 1975 High-lift aerodynamics. *J. Aircraft* **12** (6), 501–530.

TENNEKES, H. & LUMLEY, J. L. 1972 *A First Course in Turbulence*. MIT Press.

THOMAS, F. O. & LIU, X. 2004 An experimental investigation of symmetric and asymmetric turbulent wake development in pressure gradient. *Phys. Fluids* **16** (5), 1725–1745.

WYGNANSKI, I., CHAMPAGNE, F. & MARASLI, B. 1986 On the large-scale structures in two-dimensional, small-deficit, turbulent wakes. *J. Fluid Mech.* **168**, 31–71.